

INFLUENCE OF APOLIPOPROTEIN (APO) A-I STRUCTURE ON NASCENT HIGH DENSITY LIPOPROTEIN (HDL) PARTICLE SIZE DISTRIBUTION

Charulatha Vedhachalam, Palaniappan Sevugan Chetty, Margaret Nickel, Padmaja Dhanasekaran, Sissel Lund-Katz, George H. Rothblat and Michael C. Phillips*

Lipid Research Group, Gastroenterology, Hepatology and Nutrition Division, Children's Hospital of Philadelphia, University of Pennsylvania School of Medicine, Philadelphia, PA 19104-4318

Running Title: ApoA-I and Nascent HDL

* To whom correspondence should be addressed: Dr. Michael C. Phillips, The Children's Hospital of Philadelphia, Abramson Research Center, Suite 1102, 3615 Civic Center Blvd., Philadelphia, PA 19104-4318, Tel: 215-590-0587, Fax: 215-590-0583, Email: phillipsmi@email.chop.edu

SUMMARY

The principal protein of high-density lipoprotein (HDL), apolipoprotein (apo) A-I, in the lipid-free state contains two tertiary structure domains comprising an N-terminal helix bundle and a less organized C-terminal domain. It is not known how the properties of these domains modulate the formation and size distribution of apoA-I-containing nascent HDL particles created by ATP-binding cassette transporter A1(ABCA1)-mediated efflux of cellular phospholipid and cholesterol. To address this issue, proteins corresponding to the two domains of human apoA-I (residues 1-189 and 190-243) and mouse apoA-I (residues 1-186 and 187-240) together with some human/mouse domain hybrids were examined for their abilities to form HDL particles when incubated with either ABCA1-expressing cells or phospholipid multilamellar vesicles (MLV). Incubation of human apoA-I with cells gave rise to two sizes of HDL particles (8 and 10 nm hydrodynamic diameter) and removal or disruption of the C-terminal domain eliminated the formation of the smaller particle. Variations in apoA-I domain structure and physical properties exerted similar effects on the rates of formation and sizes of HDL particles created by either spontaneous solubilization of phospholipid MLV or ABCA1-mediated efflux of cellular lipids. It follows that the sizes of nascent HDL particles are determined at the point at which cellular phospholipid and cholesterol are solubilized by apoA-I; apparently, this is the rate-determining step in the overall ABCA1-mediated cellular lipid efflux process. The stability of the apoA-I N-terminal helix bundle domain and the hydrophobicity of the C-terminal domain are

important determinants of both nascent HDL particle size and their rate of formation.

INTRODUCTION

HDL particles play an anti-atherogenic role in that the level of circulating HDL is inversely associated with the risk of cardiovascular disease (1). An important way in which HDL is cardioprotective is that it promotes the reverse cholesterol transport (RCT) pathway (2), the first step in which involves HDL-mediated efflux of cholesterol from cells in the periphery (3-5). Plasma HDL comprises a heterogeneous mixture of particles of various sizes (6-7) that have differing functionalities. For instance, the inverse association between HDL cholesterol level and coronary atherosclerosis is stronger for the larger HDL₂ particles than for the smaller HDL₃ particles (8-9). It follows that it is important to understand the origins of HDL heterogeneity and, while the influence of particle remodeling in plasma is appreciated, the influence of nascent HDL particle heterogeneity is not well understood.

HDL particle biogenesis involves an interaction between the ATP binding cassette transporter A1 (ABCA1) and apolipoprotein (apo) A-I, the principal protein of HDL (10-12). This reaction involves the recruitment of cellular phospholipids (PL) and free (unesterified) cholesterol (FC) to interact with apoA-I and form nascent HDL particles. This reaction occurs at the cell surface (13-14) and the rate-limiting step is the microsolvubilization of membrane lipids to form discoidal HDL particles in the extracellular medium (15). Studies from several laboratories using various cell types have established that the nascent HDL particle population is heterogeneous (16-22). Various sized discoidal HDL particles (hydrodynamic diameters in the range 7-20nm) are created concurrently (20-21). Furthermore, these

particles are heterogeneous with respect to lipid composition, apparently reflecting the activity of ABCA1 molecules in different membrane microenvironments (16,20). Not surprisingly, the size of a discoidal HDL particles is dependent upon the number of apoA-I molecules located in it; smaller discs contain two apoA-I molecules and larger particles contain up to four apoA-I molecules. In addition to these quaternary structure effects, the tertiary structure of apoA-I (and other apolipoproteins that interact with ABCA1 to form HDL particles) is also likely to play a role. Heretofore, this issue has not been investigated systematically, although it is known that human and mouse apoA-I give rise to different sizes of HDL particles in mice (23). Here, we exploit the known differences in the tertiary structure domain properties of human and mouse apoA-I (24) to elucidate the contributions of the N-terminal helix bundle domain and the separately folded C-terminal domain (25) to ABCA1-mediated efflux of cellular cholesterol and the determination of nascent HDL particle size heterogeneity.

EXPERIMENTAL PROCEDURES

Materials

Fetal bovine serum, gentamycin, 8-(4-chlorophenylthio)-cAMP and cholesterol were purchased from Sigma-Aldrich (Boston, MA). 1-2-[³H]Cholesterol (51 Ci/mmol) was obtained from Perkin Elmer Life Sciences. Minimum essential medium (MEM) buffered with 25mM Hepes, pH 7.4 (MEM-Hepes), was obtained from BioWhittaker (Walkersville, MD). Cell culture media (RPMI 1640, DMEM) and phosphate-buffered saline were purchased from Mediatech CellGro (Manassas, VA). Tissue culture plastic wares were obtained from Falcon (Becton Dickinson Labware, Lincoln, NJ) and from Corning Inc. (Corning, NY). BSA was obtained from Celliance (Boston, MA). Acyl-CoA:cholesterol acyltransferase inhibitor (ACAT inhibitor), compound CP113, 818, was kindly provided by Pfizer Pharmaceuticals (Groton, CT). Goat polyclonal anti-human apoA-I antibody was obtained from Novus Biologicals (Littleton, CO) and rabbit anti-mouse apoA-I was purchased from Bioriginal (Saco, ME). Dimyristoyl phosphatidylcholine (DMPC), egg yolk phosphatidylcholine (PC) and porcine brain

sphingomyelin (SM) were obtained from Avanti Polar Lipids (Alabaster, AL).

Methods

Preparation of ApoA-I Variants

To express WT human apoA-I and engineered variants, the cDNA of interest was cloned into the multiple cloning sites of the pET32a (+) vector and the resulting plasmids were transformed into *Escherichia coli* strain BL21 (DE3). The target protein was expressed as a histidine-tagged fusion protein with the 109-amino acid thioredoxin (Trx) at the amino terminus (25-26).. The transformed DE3 cells were cultured in LB medium at 37°C and expression of the Trx-apoA-I fusion protein was induced with isopropyl-β-D-thiogalactopyranoside for 3 h. After sonicating the bacterial pellet, the lysate was centrifuged and the supernatant loaded onto a nickel-chelating, histidine-binding resin column (Novagen, Carlsbad, CA). The Trx-apoA-I fusion protein bound to the column was eluted, pooled, and dialyzed against 20mM NH₄HCO₃. Subsequently, the fusion protein was complexed with DMPC to prevent non-specific cleavage, and then cleaved with thrombin to release the Trx. The mixture was then lyophilized, delipidated, and dissolved in nickel-chelating column binding buffer containing 6M urea, and passed down the nickel-chelating column again. The target apoA-I was obtained in the column flow-through solution and, if needed, further purification (>95%) of the proteins was done by gel filtration with Superdex 75 and/or anion exchange chromatography with Q-Sepharose. Purity was confirmed by SDS-PAGE (not shown). All proteins were stored at -20°C in lyophilized form and before use were dissolved in the appropriate buffer containing 6M GdnHCl and dialyzed extensively.

The following human apoA-I variants (25) were used in this study: the N-terminal domain residues 1-189, the C-terminal domain residues 190-243, the C-terminal truncation variant 1-222, the point mutant L230P and triple mutant L230PL233PY236P, and the deletion mutants Δ44-126 and Δ123-166. The following mouse apoA-I variants (24,27) were also employed: WT mouse apoA-I, the N-terminal domain residues 1-186, and the C-terminal domain residues 187-240. In addition, human(H)/mouse(M) apoA-I hybrid molecules in which the N- and C-terminal

domains were swapped (24) were utilized: H1-189M187-240 and M1-186H190-243.

Cholesterol efflux from cells

J774 murine macrophages were grown and maintained in RPMI 1640 supplemented with 10% fetal bovine serum and 0.5% gentamycin, as described before (28). For cholesterol efflux experiments, these cells were then seeded in 12-well plates and grown to 80-90% confluence. They were then labeled by incubating the cells for 24 h in RPMI medium supplemented with 1% fetal bovine serum, 2 $\mu\text{g/ml}$ CP-113,818 ACAT inhibitor and 3 $\mu\text{Ci/ml}$ [^3H]cholesterol. After labeling, the cells were washed with MEM-Hepes and incubated with RPMI medium containing 0.2% (w/v) bovine serum albumin, 2 $\mu\text{g/ml}$ CP-113,818 ACAT inhibitor, and 0.3 mM 8-(4-chlorophenylthio)-cAMP for 12 h, to up-regulate the expression of ABCA1. Cells were then washed with MEM-Hepes and incubated with or without WT or mutant apoA-I at the indicated concentrations for 4 h. To determine FC efflux, aliquots were removed from the incubation medium at specific time points, filtered and radioactivity was determined by liquid scintillation counting. The percent FC efflux was calculated after subtracting the background FC efflux (without apoA-I) as follows: (counts/min in medium at 4 h/cpm in cells at $t = 0$) \times 100. K_m and V_{max} values were calculated by fitting the fractional lipid efflux values obtained at 4 h and different concentrations of apoA-I to the Michaelis-Menten equation (Graphpad Prism).

BHK cells expressing high levels of human ABCA1 (29-30) (kindly provided by Dr. John Oram) were grown and maintained in DMEM containing 10% FBS and 0.5% gentamicin. For efflux experiments, these cells were seeded in 12-well plates and then labeled by incubating the cells for 24 h in DMEM medium supplemented with 2.5% fetal bovine serum, 2 $\mu\text{g/ml}$ CP-113, 818 ACAT inhibitor and 3 $\mu\text{Ci/ml}$ [^3H]cholesterol. ABCA1 was induced by incubating the labeled cells for 18 h in DMEM containing 0.2% BSA and 10 nM mifepristone. Cells were then washed with MEM-Hepes and incubated with or without WT or mutant apoA-I under the indicated conditions of concentration for 4 h and the cholesterol efflux was determined as described above.

Characterization of nascent HDL

The conditioned medium from J774 and BHK ABCA1-expressing cells exposed to 10 $\mu\text{g/ml}$ apoA-I was fractionated by gel filtration chromatography on a calibrated Superdex 200 column, as described before (16,20,22). Nondenaturing 4-12% gradient gel (Invitrogen, Carlsbad, CA) electrophoresis was also used to separate nascent apoA-I-containing HDL particles, and the gels were immunoblotted for apoA-I (20,31). The methods for determining the concentrations of protein and cholesterol have been reported previously (20).

Lipid solubilization assay

Appropriate amounts of DMPC and cholesterol (5 mol %) in chloroform were dried, dispersed in Tris-buffered saline (pH 7.4) with vortexing and subjected to three temperature cycles between 0 and 37°C to ensure complete hydration. The resultant multilamellar vesicles (MLV) were incubated at a 2/1 w/w lipid/protein ratio with apoA-I for 20 h at 26°C. Mixtures of 1/9 w/w egg PC/porcine brain SM were prepared similarly and dispersed in buffer by vortexing followed by water-bath sonication for 30 minutes at room temperature. The resultant MLV (2 mg PL/ml) were incubated at a 1/2 w/w lipid/protein ratio with apoA-I for 18 h at 37°C. The size-distributions of the discoidal HDL particles created (32-33) were analyzed by native 4-12% and 4-20% PAGE.

RESULTS

Contributions of apoA-I tertiary structure domains to FC efflux

As we have reported before (28), the ABCA1-mediated efflux of FC from ABCA1-expressing J774 cells exhibits a hyperbolic dependence on the concentration of human apoA-I in the extracellular medium and conforms to the Michaelis-Menten equation (Fig. 1A). The V_{max} and K_m values listed in Table 1 for WT apoA-I(H) are similar to previous values (28). The isolated N-terminal domain of human apoA-I is less effective at supporting FC efflux (Fig. 1A) and the relative catalytic efficiency (V_{max}/K_m) decreases from 1.0 for WT apoA-I(H) to 0.3 for apoA-I 1-189(H) (Table 1). This result is consistent with the well-established finding that the C-terminal of the apoA-I molecule is critical for effective ABCA1-

mediated FC efflux to apoA-I (16,34-39). Surprisingly, despite its high lipid affinity (24), the isolated C-terminal domain of human apoA-I, apoA-I 190-243(H), is not particularly effective (relative catalytic efficiency 0.4, Table 1). Replotting Fig. 1A so the apoA-I domain concentrations are expressed in molar terms (data not shown) shows that the sum of the efflux contributions of the isolated N- and C-terminal domain fragments is less than the efflux observed with the equivalent concentration of intact WT apoA-I. This result implies that the N- and C-terminal domains cooperate to enhance FC efflux to human apoA-I via ABCA1.

The altered N- and C-terminal tertiary domain structures in mouse apoA-I compared to human apoA-I lead to variations in FC efflux via ABCA1. Thus, WT mouse apoA-I is less effective than human apoA-I (Fig. 1B) and the relative catalytic efficiency is 0.6 for WT apoA-I(M) (Table 1). This decreased efflux efficiency occurs even though there is no species disparity between mouse apoA-I and J774 cells that express the murine ABCA1 transporter. In marked contrast to the situation with human apoA-I (Fig. 1A), the isolated mouse N-terminal helix bundle domain apoA-I 1-186(M) is much more effective at promoting FC efflux than the intact mouse apoA-I molecule (Fig. 1B). This effect is demonstrated by the increase in relative catalytic efficiency to a value of 4.4 for apoA-I 1-186(M) (Table 1); this value is approximately 7- and 4-fold higher than the values for WT mouse and human apoA-I, respectively. The isolated mouse apoA-I C-terminal domain, apoA-I 187-240(M), fails to promote FC efflux (Fig. 1B) which is consistent with the high polarity and poor lipid-binding abilities of this domain (24).

The results in Fig. 2 and Table 1 for FC efflux from BHK cells (which express human ABCA1) to the same human and mouse apoA-I domains reveal similar trends to those described above for experiments with J774 cells. It follows that mouse and human ABCA1 respond similarly to alterations in apoA-I structure. Again, the data in Fig. 2A indicate that the contributions of the two tertiary structure domains in the intact human apoA-I molecule are greater than their combined contributions when added separately to the cells. Fig. 2B demonstrates that the isolated mouse N-terminal domain, apoA-I 1-186(M), is more

efficient at promoting FC efflux than WT mouse apoA-I.

Human/mouse hybrid apoA-I molecules in which the N- and C-terminal domains are interchanged were employed to further investigate the domain contributions to FC efflux via ABCA1. Substituting the mouse C-terminal domain into human apoA-I to create apoA-I H1-189M187-240 has little effect on FC efflux from J774 cells (Fig. 3A and Table 1). However, the increase in K_m for efflux from BHK cells (Fig. 3B) reduces the relative catalytic efficiency to a value of 0.25 (Table 1); the reasons for this effect are not entirely clear but perhaps the composition of the BHK cell plasma membrane makes the system more sensitive to the increase in polarity of the C-terminal domain in the hybrid human apoA-I molecule. Substitution of the human C-terminal domain into the mouse apoA-I molecule, to give the hybrid apoA-I M1-186H190-243, increases the relative catalytic efficiency approximately 3-fold relative to WT apoA-I(M) and approximately 2-fold relative to WT apoA-I(H) for both cell types (Table 1).

Nascent HDL particle size distribution

The gel filtration profiles in Fig. 4A confirm prior work with J774 murine macrophages showing that the apoA-I(H)/ABCA1 reaction in this system leads to the appearance in the extracellular medium of a heterogeneous population of apoA-I-containing nascent HDL particles (16,20). In addition, cholesterol is released from the cells in larger microparticles (diameter >20nm) that elute in the void volume of the Superdex 200 column (16,20,40); these particles do not contain any apoA-I. WT apoA-I(H) produces two main populations of HDL particles with hydrodynamic diameters of 8-9 and 12nm (Fig. 4A). In contrast, WT apoA-I(M) produces a more heterogeneous population of larger HDL particles that elute as single peak with a maximum corresponding to a diameter of approximately 13nm (Fig. 4B). The difference in size distribution of nascent HDL particles containing either human or mouse apoA-I (Fig. 4) is probably responsible for the differences in plasma HDL that occur in transgenic mice expressing human apoA-I. Replacement of apoA-I(M) with apoA-I(H) leads to the single 9.5nm HDL species present in the plasma of control mice

being replaced by two HDL subclasses with diameters of ~ 8.5 and 10.5nm (23).

More extensive characterization of the influence of apoA-I domain structure on nascent HDL particle size distribution was conducted with BHK cells expressing human ABCA1 because FC efflux and HDL particle production is greater with these cells compared to J774 cells (Table 1). In agreement with results in Fig. 4 for J774 cells, the data in Fig. 5A, D for WT apoA-I(H) and WT apoA-I(M), respectively, show that in the BHK cell system the former protein forms two major subclasses of HDL particles (diameters of 8 and 10nm) (in agreement with a prior report with these BHK cells (41)) whereas the latter protein forms a single population of ~11nm diameter. For both apoA-I(H) and apoA-I(M), removal of the C-terminal domain to give the isolated N-terminal helix bundle domain leads to a single peak of larger HDL (Fig. 5A, D). In the case of apoA-I(H), deletion of the C-terminal domain prevents formation of the smaller 8nm subpopulation of HDL particles. Interestingly, the isolated human C-terminal domain (190-243(H)) forms only the 10nm population. Thus, both domains in apoA-I(H) are needed for two subpopulations of HDL particles to be created. The data in Fig. 5B, C show that structural alterations in either the N- or C-terminal domains can modulate nascent HDL particle size. Thus, either deletion of the C-terminal helix (residues 223-243) (cf. (16)) or disruption of helix formation by proline insertion (L230P, L230PL233PY236P) prevents formation of two discrete populations of HDL particles and causes a single more disperse and larger population centered at ~13nm to be formed (Fig. 5B). Disruption of the helix bundle domain (deletion mutants Δ 123-166, Δ 44-126) also induces alterations in HDL particle size distribution; in this case, the principal effect is reduction in the formation of the 8nm particles with 9-10nm particles predominating (Fig. 5C). Overall, these results demonstrate that native human N- and C-terminal domains are needed for formation of the 8 and 10nm HDL subpopulations. The differences in structures of both domains in apoA-I(M) compared to apoA-I(H) (24) are sufficient to eliminate formation of the two populations, and permit only the larger particle size distribution.

To further resolve the nascent HDL particle size distribution, we used native 4-12% PAGE which resolves HDL particles better than Superdex 200 gel filtration chromatography. Lane 1 of the gel shown in Fig. 6 confirms the gel filtration profile in Fig. 5A and demonstrates that WT apoA-I(H) forms 8 and 10nm particles (the band close to 7.1nm is due to lipid-free apoA-I). The gel in Lane 2 confirms that the isolated human N-terminal domain (1-189(H)) forms a broader distribution of larger HDL particles, with the appearance of a band at close to 17nm. Comparison of Lanes 1 and 3 shows that the distribution of nascent HDL particles formed by WT apoA-I(M) is skewed to larger sizes relative to WT apoA-I(H). The gel in Lane 4 is consistent with the gel filtration profiles in Fig. 5D in showing that the isolated helix bundle domain from apoA-I(M) forms a population of relatively large HDL particles compared to WT apoA-I(M). Gels corresponding to the elution profiles for the several apoA-I variants described in Fig. 5B, C could not be obtained because of the lack of appropriate anti-apoA-I antibodies.

The human/mouse domain swap hybrid apoA-I molecules were utilized to further investigate the influence of the apoA-I N- and C-terminal domains on nascent HDL particle formation. Fig. 7A shows that replacement of the human C-terminal domain with the mouse counterpart to give H1-189M186-240 reduces formation of the 8nm HDL particle; a population of larger particles with a peak diameter of 11nm is formed. As can be seen from Fig. 7B, this particle size distribution is similar to that created by WT apoA-I(M). Fig. 7B also demonstrates that the human C-terminal domain is required for efficient formation of the 8nm HDL particle population because, like WT apoA-I(H), the apoA-I hybrid M1-186-H190-243 forms well resolved 8 and 10nm particles. The hydrodynamic diameters of the predominant nascent HDL species (from gel filtration profiles in Fig. 5 and 7) formed when the apoA-I variants with different domains are incubated with BHK cells are summarized in Table 2. The effects of apoA-I domain structure on nascent HDL particle size are not dependent upon cell type because the same phenomena were observed with J774 cells (data not shown).

ApoA-I domain structure and sizes of HDL particles created by solubilization of PL

Since ABCA1-mediated formation of HDL particles involves solubilization of plasma membrane lipids by apoA-I (15), we examined the concept of whether or not apoA-I structural domains have similar effects on the size distribution of HDL particles formed when apoA-I solubilizes either DMPC/cholesterol or egg PC/porcine brain SM bilayers in the absence of ABCA1.

Under the conditions employed, the DMPC/5 mol % cholesterol complexes formed by WT apoA-I(H) migrate as a doublet (diameter ~10.4nm) and a separate band corresponding to a diameter of ~13nm (Fig. 8A, Lane 2). Lanes 3 and 4 in the same gel show that, as with ABCA1-mediated formation of HDL particles (Fig. 5A), the smaller ~10.4nm particles do not form and larger particles (diameter ~16-18 nm) are created when the isolated N- and C-terminal domains of apoA-I(H) solubilize DMPC. Consistent with the ABCA1 case (Fig. 4A, B and Fig. 5 A, D), compared to apoA-I(H), mouse apoA-I creates a broader range of particles that is skewed towards a diameter of ~17nm (cf. Lane 2 in Fig. 8A and Lane 1 in Fig. 8B). The isolated N-terminal domains of human and mouse apoA-I both form a relatively homogenous population of particles migrating between the 12.1-17.0 nm standards (Fig. 8A, Lane 3 and Fig. 8B, Lane 2). Exchange of the mouse C-terminal domain into apoA-I(H) to give H1-189M187-240 favors formation of large apoA-I/DMPC particles (Fig. 8A, Lane 5), which is similar to the shift in equivalent gel filtration profiles obtained with BHK cell-conditioned medium (Fig. 7A). However, unlike the case of the nascent HDL particles created by interaction with ABCA1 (Fig. 7B), insertion of the human C-terminal domain into apoA-I(M) to give M1-186H190-243 (Fig. 8B, Lane 3), while favoring formation of smaller HDL particles (diameter ~9nm), does not give an HDL particle distribution like that of WT apoA-I(H) (Fig. 8A, Lane 2).

To confirm that the above effects of apoA-I structure on the sizes of HDL particles created by the solubilization of MLV are not peculiar to the DMPC system, similar experiments were conducted with MLV of egg PC/porcine brain SM and the results are shown in Fig. 8 C, D. In agreement with prior work (33,42), solubilization

of MLV containing SM leads to the formation of relatively large discoidal HDL particles (cf. Fig. 8C, D to Fig. 8A, B). Importantly, the effects of apoA-I domain structure variation on the relative sizes of HDL particles formed by spontaneous solubilization of egg PC/porcine brain SM MLV are similar to the effects seen with the DMPC/cholesterol system. Thus, the contributions of apoA-I tertiary domain structure to HDL particle size are apparently similar, regardless of the precise composition of the PL MLV being solubilized.

DISCUSSION

In the three-step reaction by which apoA-I and ABCA1 promote the efflux of cellular lipid and create nascent HDL particles, the last step involving the solubilization by apoA-I of plasma membrane PL and FC is apparently rate-limiting (15). This microsolvubilization process requires insertion of apoA-I amphipathic helices between the plasma membrane PL molecules and bilayer fragmentation to create discoidal HDL particles (15,36). A more complete mechanistic understanding of these effects requires knowledge of the influence of apoA-I tertiary structure domain properties on the rates of PL and FC efflux, and on the assembly of nascent HDL particles. The present investigation provides insight into the influences of N-terminal helix bundle stability and C-terminal domain hydrophobicity on ABCA1-mediated cellular lipid efflux and HDL particle biogenesis.

FC Efflux

Figure 9 shows that for the human and mouse apoA-I variants studied there is a strong correlation ($r^2 = 0.80$) between their effects on the kinetics of cellular FC efflux via ABCA1 and solubilization of DMPC/cholesterol vesicles. The fact that alterations in apoA-I domain properties have similar effects on the two processes supports the idea that the rate-limiting event in the ABCA1 reaction is the final step of solubilization of plasma membrane PL and FC to create discoidal nascent HDL particles (15). Since the isolated C-terminal domain of apoA-I (H) (190-243)(H) promotes significant efflux from BHK cells whereas the equivalent mouse apoA-I domain (187-240(M)) is inactive (Table 1 and Fig. 2), it is clear that the helix content and polarity of this domain are important; the C-terminal domain of

apoA-I (H) is known to be more helical and contain more hydrophobic amino acid residues than the equivalent domain in apoA-I (M) (24). The important contribution of the hydrophobicity and lipid-solubilizing capability of the C-terminal domain to the functionality of WT apoA-I (H) is further demonstrated by the fact that its deletion to give apoA-I 1-189(H) reduces the relative catalytic efficiency of efflux by 60% (Table 1). In support of the key role played by C-terminal domain hydrophobicity, elimination of the polar (and non-lipid binding) C-terminal domain of WT mouse apoA-I does not lead to a reduction of FC efflux; in fact the relative catalytic efficiency of FC efflux is more than doubled (Table 1). The properties of the apoA-I N-terminal helix bundle domain are also significant for FC efflux because the relative catalytic efficiency of apoA-I 1-186 (M) is four times greater than that of apoA-I 1-189 (H) (Table 1). The major difference between the N-terminal domains of human and mouse apoA-I is the lower stability of the helix bundle in the latter protein; the amino acid sequences in this domain are 70% identical (43) but the helix content is lower in the mouse helix bundle and the mid-point of thermal denaturation is 41°C as compared to 51°C for the human helix bundle domain (24). A reduction in helix bundle stability is expected to enhance FC efflux because the rate of lipid solubilization is increased due to the greater time-average exposure of hydrophobic surface area facilitating penetration of amphipathic helices into the PL bilayer (44).

In the intact WT apoA-I molecules, interplay between the properties of the N- and C-terminal domains modulates overall functionality in FC efflux. Thus, WT apoA-I (H) is effective because the contribution from the hydrophobic C-terminal domain overrides the poor ability of the relatively stable N-terminal helix bundle domain to solubilize lipids (thereby decreasing the K_m relative to the value for apoA-I 1-189(H), Table 1). In contrast, the polar C-terminal domain in apoA-I (M) hinders the high ability of the unstable helix bundle domain to solubilize lipids and promote FC efflux (as reflected in the higher K_m (Table 1) for WT apoA-I (M) compared to apoA-I 1-186 (M)). The interplay between the contributions of the N- and C-terminal domains to the functionality of the intact apoA-I molecule is further exemplified by the results for the

human/mouse hybrid apoA-I molecules. Thus, insertion of the polar mouse C-terminal domain into apoA-I (H) to give apoA-I H1-189 M187-240 reduces efflux (the relative catalytic efficiency with BHK cells decreases by a factor of four due to an increase in K_m – Table 1). In marked contrast, insertion of the hydrophobic human C-terminal domain into apoA-I (M) to yield apoA-I M1-186 H190-243 decreases the K_m and increases the relative catalytic efficiency from 0.7 to 1.7. The behavior of this hybrid apoA-I molecule shows that the combination of an unstable helix bundle and a hydrophobic C-terminal domain elevates functionality.

Overall, the studies of the contributions of apoA-I domain properties to FC efflux via ABCA1 suggest that the efficacy of WT apoA-I (H) can be improved by engineering into the molecule some destabilization of the helix bundle together with increased hydrophobicity of the C-terminal domain. The contributions of the two domains are enhanced when they are covalently linked in an intact apoA-I molecule rather than being present separately.

Nascent HDL Particle Distribution

Analysis of the nascent HDL particles existing after the apoA-I variants are incubated with BHK cells (Table 2) indicates that the two populations of 8 and 10nm particles are formed only in the presence of a full-length apoA-I molecule containing the hydrophobic human C-terminal domain (i.e. WT apoA-I(H) or apoA-I M 1-186 H190-243). Removal of the C-terminal domain from apoA-I leads to formation of larger HDL particles that elute from the Superdex 200 gel filtration column as a single peak. Similarly, removal of the C-terminal domain from apoA-I (H) prevents formation of smaller particles when PL MLV are solubilized (Fig. 8A and C), and insertion of this domain into apoA-I(M) gives rise to smaller HDL particles (cf. lane 3 to lane 1 in Fig. 8B and 8D). In sum, these results show that the various apoA-I structural domains exert similar effects on the sizes of the HDL particles whether they are created either by the ABCA1 reaction or by direct PL MLV solubilization. These findings are consistent with the PL bilayer solubilization step being the point in the ABCA1-mediated reaction where the sizes of the nascent HDL particles are determined.

How do the properties of the apoA-I N- and C-terminal domains modulate the lipid solubilization process and alter HDL particle size distribution? Apparently, kinetic effects are not a factor because there is no correlation between the rate of FC efflux from BHK cells to the apoA-I variants (Table 1) and the sizes of the resultant nascent HDL particle (Table 2). As an example of this lack of a kinetic effect, the helix bundle domain of the mouse protein, apoA-I 1-186(M) reacts rapidly to form larger HDL particles while the human counterpart, apoA-I 1-189(H), also forms larger particles but reacts relatively slowly. As mentioned above, in the systems studied here the hydrophobic human C-terminal domain is required for formation of the population of small 8nm nascent HDL particles. A possible explanation for this effect is that the high affinity of this domain for the surface of a PL bilayer vesicle causes a high surface concentration of

apoA-I molecules to be attained. If this condition is accompanied by deeper penetration of more amphipathic helices into the PL bilayer (36) then, when the bilayer becomes sufficiently destabilized, fragmentation into smaller segments may also be possible (44-45).

In conclusion, it is apparent that the tertiary structure of apoA-I influences (1) the kinetics of ABCA1-mediated efflux of cellular PL and FC, and (2) HDL heterogeneity by modulating the size distribution of the nascent particles created. The presence of the hydrophobic C-terminal domain in apoA-I(H) favors formation of smaller nascent HDL particles relative to the particles created by apoA-I(M). This particular property of the human C-terminal domain may be significant for HDL function because the anti-atherogenic properties of HDL are apparently influenced by particle size (8-9).

REFERENCES

1. Castelli, W. P. (1984) *American Journal of Medicine* 76, 4-12
2. Cuchel, M., and Rader, D. J. (2006) *Circulation* 113, 2548-2555
3. Johnson, W. J., Mahlberg, F. H., Rothblat, G. H., and Phillips, M. C. (1991) *Biochim.Biophys.Acta* 1085, 273-298
4. Yancey, P. G., Bortnick, A. E., Kellner-Weibel, G., de la Llera-Moya, M., Phillips, M. C., and Rothblat, G. H. (2003) *Arterioscler.Thromb.Vasc.Biol.* 23, 712-719
5. Tall, A. R. (2008) *J.Internal Med.* 263, 256-273
6. Lund-Katz, S., Liu, L., Thuahnai, S. T., and Phillips, M. C. (2003) *Frontiers in Bioscience* 8, d1044-1054
7. Jonas, A., and Phillips, M. C. (2008) Lipoprotein Structure. in *Biochemistry of Lipids, Lipoproteins and Membranes* (Vance, D. E., and Vance, J. E. eds.), Elsevier. pp 485-506
8. Miller, N. E. (1987) *Am Heart J* 113, 589-597
9. Drexel, H., Amann, F. W., Rentsch, K., Neuenschwander, C., Luethy, A., Khan, S. I., and Follath, F. (1992) *Am J Cardiol* 70, 436-440
10. Lee, J. Y., and Parks, J. S. (2005) *Curr.Opin.Lipidol.* 16, 19-25
11. Oram, J. F., and Heinecke, J. W. (2005) *Physiol.Rev.* 85, 1343-1372
12. Yokoyama, S. (2006) *Arterioscler.Thromb.Vasc.Biol.* 26, 20-27
13. Faulkner, L. E., Panagotopulos, S. E., Johnson, J. D., Woollett, L. A., Hui, D. Y., Witting, S. R., Maiorano, J. N., and Davidson, W. S. (2008) *J.Lipid Res.* 49, 1322-1332
14. Denis, M., Landry, Y. D., and Zha, X. (2008) *J.Biol.Chem.* 283, 16178-16186
15. Vedhachalam, C., Duong, P. T., Nickel, M., Nguyen, D., Dhanasekaran, P., Saito, H., Rothblat, G. H., Lund-Katz, S., and Phillips, M. C. (2007) *J.Biol.Chem.* 282, 25123-25130
16. Liu, L., Bortnick, A. E., Nickel, M., Dhanasekaran, P., Subbaiah, P. V., Lund-Katz, S., Rothblat, G. H., and Phillips, M. C. (2003) *J.Biol.Chem.* 278, 42976-42984
17. Denis, M., Haidar, B., Marcil, M., Bouvier, M., Krimbou, L., and Genest, J., Jr. (2004) *J.Biol.Chem.* 279, 7384-7394
18. Krimbou, L., Denis, M., Haidar, B., Carrier, M., Marcil, M., and Genest, J., Jr. (2004) *J.Lipid Res.* 45, 839-848
19. Krimbou, L., Hassan, H. H., Blain, S., Rashid, S., Denis, M., Marcil, M., and Genest, J. (2005) *J.Lipid Res.* 46, 1668-1677
20. Duong, P. T., Collins, H. L., Nickel, M., Lund-Katz, S., Rothblat, G. H., and Phillips, M. C. (2006) *J.Lipid Res.* 47, 832-843
21. Mulya, A., Lee, J. Y., Gebre, A. K., Thomas, M. J., Colvin, P. L., and Parks, J. S. (2007) *Arterioscler.Thromb.Vasc.Biol.* 27, 1828-1836
22. Duong, P. T., Weibel, G. L., Lund-Katz, S., Rothblat, G. H., and Phillips, M. C. (2008) *J.Lipid Res.* 49, 1006-1014
23. Rubin, E. M., Ishida, B. Y., Clift, S. M., and Krauss, R. M. (1991) *Proc.Natl.Acad.Sci.USA* 88, 434-438
24. Tanaka, M., Koyama, M., Dhanasekaran, P., Nguyen, D., Nickel, M., Lund-Katz, S., Saito, H., and Phillips, M. C. (2008) *Biochemistry* 47, 2172-2180
25. Saito, H., Dhanasekaran, P., Nguyen, D., Holvoet, P., Lund-Katz, S., and Phillips, M. C. (2003) *J.Biol.Chem.* 278, 23227-23232
26. Morrow, J. A., Arnold, K. S., and Weisgraber, K. H. (1999) *Protein Expr.Purif.* 16, 224-230
27. Koyama, M., Tanaka, M., Dhanasekaran, P., Lund-Katz, S., Phillips, M. C., and Saito, H. (2009) *Biochemistry* 48, 2529-2537
28. Vedhachalam, C., Liu, L., Nickel, M., Dhanasekaran, P., Anantharamaiah, G. M., Lund-Katz, S., Rothblat, G., and Phillips, M. C. (2004) *J.Biol.Chem.* 279, 49931-49939
29. Oram, J. F., Vaughan, A. M., and Stocker, R. (2001) *J Biol Chem* 276, 39898-39902
30. Vaughan, A. M., and Oram, J. F. (2003) *J.Lipid.Res.* 44, 1373-1380

31. Alexander, E. T., Tanaka, M., Kono, M., Saito, H., Rader, D. J., and Phillips, M. C. (2009) *J Lipid Res* 50, 1409-1419
32. Massey, J. B., and Pownall, H. J. (2008) *Biochim.Biophys.Acta* 1781, 245-253
33. Fukuda, M., Nakano, M., Sriwongsitanont, S., Ueno, M., Kuroda, Y., and Handa, T. (2007) *J.Lipid Res.* 48, 882-889
34. Sviridov, D., Pyle, L. E., and Fidge, N. (1996) *J.Biol.Chem.* 271, 33277-33282
35. Burgess, J. W., Frank, P. G., Franklin, V., Liang, P., McManus, D. C., Desforges, M., Rassart, E., and Marcel, Y. L. (1999) *Biochemistry* 38, 14524-14533
36. Gilotte, K. L., Zaiou, M., Lund-Katz, S., Anantharamaiah, G. M., Holvoet, P., Dhoest, A., Palgunachari, M. N., Segrest, J. P., Weisgraber, K. H., Rothblat, G. H., and Phillips, M. C. (1999) *J.Biol.Chem.* 274, 2021-2028
37. Panagotopoulos, S. E., Witting, S. R., Horace, E. M., Hui, D. Y., Maiorano, J. N., and Davidson, W. S. (2002) *J.Biol.Chem.* 277, 39477-39484
38. Favari, E., Bernini, F., Tarugi, P., Franceschini, G., and Calabresi, L. (2002) *Biochem.Biophys.Res.Comm.* 299, 801-805
39. Chroni, A., Liu, T., Gorshkova, I., Kan, H. Y., Uehara, Y., von Eckardstein, A., and Zannis, V. I. (2003) *J.Biol.Chem.* 278, 6719-6730
40. Nandi, S., Ma, L., Denis, M., Karwatsky, J., Li, Z., Jiang, X. C., and Zha, X. (2009) *J Lipid Res* 50, 456-466
41. Vaughan, A. M., and Oram, J. F. (2006) *J.Lipid Res.* 47, 2433-2443
42. Swaney, J. B. (1983) *J Biol Chem* 258, 1254-1259
43. Brouillette, C. G., Anantharamaiah, G. M., Engler, J. A., and Borhani, D. W. (2001) *Biochim.Biophys.Acta* 1531, 4-46
44. Segall, M. L., Dhanasekaran, P., Baldwin, F., Anantharamaiah, G. M., Weisgraber, K., Phillips, M. C., and Lund-Katz, S. (2002) *J.Lipid Res.* 43, 1688-1700
45. Pownall, H., Pao, Q., Hickson, D., Sparrow, J. T., Kusserow, S. K., and Massey, J. B. (1981) *Biochemistry* 20, 6630-6635

FOOTNOTES

Acknowledgments

We thank Dr. John Oram for his gift of BHK cells expressing human ABCA1. This research was supported by NIH Grant HL22633.

Abbreviations

ABCA1, ATP binding cassette transporter A1; apo, apolipoprotein; BHK, baby hamster kidney; DMPC, dimyristoyl phosphatidylcholine; FC, free (unesterified) cholesterol; HDL, high density lipoprotein; PC, phosphatidylcholine; PL, phospholipid; SM, sphingomyelin; Trx, thioredoxin; WT, wild type.

FIGURE LEGENDS

Figure 1: Effect of apoA-I tertiary structure domains on cholesterol efflux from J774 macrophages:

J774 macrophages were labeled with [³H] - cholesterol (3μCi/ml) and treated with cpt-cAMP to upregulate mouse ABCA1 expression. Cholesterol efflux was then initiated by the addition of apoA-I (0-20 μg/ml). After 4h incubation, the medium was removed, filtered and the [³H] - radioactivity determined. The fractional cholesterol efflux is plotted as a function of apo A-I concentration, and fitted to the Michaelis-Menten equation. Data points represent FC efflux to WT human apo A-I (■), 1-189 (H) (●), 190-243 (H) (*), (Panel A) and WT mouse apo A-I (▲), 1-186 (M) (x) and 187-240 (M) (∇) (Panel B).

Figure 2: Effect of apoA-I tertiary structure domains on cholesterol efflux from BHK cells:

BHK cells were labeled with [³H] - cholesterol and treated with mifepristone to upregulate human ABCA1 expression. Cholesterol efflux was then initiated by the addition of apoA-I (0-20 μg/ml). After 4h

incubation, the medium was removed, filtered and the [³H] - radioactivity determined. The fractional cholesterol efflux is plotted as a function of apo A-I concentration, and fitted to the Michaelis-Menten equation. Data points represent FC efflux to WT human apo A-I (■), 1-189 (H) (●), 190-243 (H) (*) (Panel A), mouse apo A-I (▲), 1-186 (M) (x) and 187-240 (M) (∇) (Panel B).

Figure 3: Cholesterol efflux from J774 and BHK cells to human/mouse hybrid apo A-I molecules: The curves for WT human (dotted line) and mouse (dot-dash line) apo A-I in Panels A and B are replotted from Fig. 1 and 2 for ease of comparison. Data points represent FC efflux to H1-189M187-240 (*) and M1-186H190-243 (∇).

Figure 4: Gel filtration elution profiles of medium collected after incubation of J774 macrophages with ¹⁴C-labeled apolipoprotein: J774 macrophages were labeled with [³H] - cholesterol and these labeled cells were incubated with 0.3mM of cpt-cAMP overnight. Efflux was initiated by the addition of 10μg/ml of either [¹⁴C]-WT human apo A-I (Panel A) or mouse apo A-I (Panel B). After 6h incubation, aliquots of the media were collected, filtered, and [³H] - labeled lipoprotein particles from cells treated with WT human (Δ) and mouse (□) apo A-I were separated by gel filtration chromatography on a calibrated Superdex 200 column. Fractions were collected and radioactivity was determined by liquid scintillation counting.

Figure 5: Gel filtration elution profiles of medium collected after incubation of BHK cells with human or mouse apo A-I: BHK cells expressing human ABCA1 were labeled with [³H] - cholesterol and efflux was initiated by the addition of 10μg/ml of apo A-I. A. WT human apo A-I (Δ), 1-189 (H) (●), 190-243 (H) (+). B. 1-222 (H) (◆), L230P (H) (*), L230PL233PY236P (H) (∇). C. Δ123-166 (H) (■), Δ44-126 (H) (◇). D. WT mouse apoA-I (x) and 1-186 (M) (○). The media were analyzed as described in the legend to Fig. 4. To avoid peak overlap in Panel A, the Y-axis unit for 190-243 (H) was cpm/0.5ml.

Figure 6: Blots stained with anti-apoA-I of native polyacrylamide gradient (4-12%) gels comparing the size distributions of the nascent HDL particles formed in the extracellular medium by incubation of apoA-I variants with ABCA1-expressing BHK cells: Lane 1, WT apoA-I (H) (Fig. 5A). Lane 2, 1-189 (H) (Fig. 5A). Lane 3, WT apoA-I (M) (Fig. 5D). Lane 4, 1-186 (M) (Fig. 5D). The migration positions of standard proteins of known hydrodynamic diameters are indicated in the two panels.

Figure 7: Gel filtration elution profiles of medium collected after incubation of BHK cells with human/mouse apo A-I domain-swap hybrids: BHK cells expressing human ABCA1 were labeled with [³H] - cholesterol and efflux was initiated by the addition of 10μg/ml of apo A-I. A. WT human apo A-I (○) and H1-189M187-240 (▲). B. mouse apo A-I (∇) and M1-186H190-243 (■). The media were analyzed as described in the legend to Fig. 4.

Figure 8: Native polyacrylamide gradient gels stained with Coomassie Brilliant Blue comparing the sizes of discoidal complexes formed by incubation of PL MLV with apoA-I variants: Panel A (4-12% gel). Human apoA-I and DMPC/5 mol % cholesterol MLV. Lane 1, standard proteins of known hydrodynamic diameters. Lane 2, WT apoA-I (H). Lane 3, 1-189 (H). Lane 4, 190-243 (H). Lane 5, H1-189M187-240. Panel B (4-12% gel). Mouse apoA-I and DMPC/5 mol % cholesterol MLV. Lane 1, WT apoA-I (M). Lane 2, 1-186(M) Lane 3, M1-186H190-243. Panel C (4-20% gel). Human apoA-I and 1/9 w/w egg PC/ porcine brain SM MLV. The designations for Lanes 1-5 are the same as in Panel A. Panel D (4-20% gel). Mouse apoA-I and 1/9 w/w egg PC/porcine brain SM MLV. The designations for Lanes 1-3 are the same as in Panel B.

Fig. 9: Correlation between the effectiveness of apoA-I tertiary structure domains in participating in ABCA1-mediated cellular cholesterol efflux and in solubilizing DMPC MLV. The values of relative catalytic efficiency (V_{max}/K_m) for cellular cholesterol efflux to apoA-I variants are for BHK cells and are taken from Table 1. The relative catalytic efficiencies for solubilization of DMPC MLV by the same apoA-I variants are computed from V_{max} and K_m values tabulated in ref (24).

Table 1 Kinetic parameters for cholesterol efflux to apoA-I from J774/BHK cells

<i>Apo-lipoprotein</i>	<i>FC efflux (J774 cells)</i>			<i>FC efflux (BHK cells)</i>		
	Relative V_{max}^a	K_m ($\mu\text{g apo/ml}$)	Relative catalytic efficiency ^b	Relative V_{max}^c	K_m ($\mu\text{g apo/ml}$)	Relative catalytic efficiency ^d
WT apoA-I (H)	1.0	5.7 ± 0.2 (n=15)	1.0	1.0	6.7 ± 0.4 (n=12)	1.0
1-189 (H)	1.8 ± 0.06 (n=6)	31.8 ± 1.7 (n=6)	0.3	1.8 ± 0.3 (n=3)	28.5 ± 6.1 (n=3)	0.4
190-243 (H)	0.8 ± 0.04 (n=6)	11 ± 1.2 (n=6)	0.4	1.4 ± 0.2 (n=3)	20.4 ± 4.0 (n=3)	0.45
WT apoA-I (M)	2.5 ± 0.04 (n=15)	24 ± 0.6 (n=15)	0.6	1.5 ± 0.1 (n=3)	14.7 ± 2.0 (n=3)	0.7
1-186 (M)	1.8 ± 0.05 (n=3)	2.3 ± 0.2 (n=3)	4.4	1.4 ± 0.1 (n=3)	5.7 ± 1.0 (n=3)	1.6
H1-189 M187-240	1.6 ± 0.1 (n=3)	9.6 ± 1.3 (n=3)	0.9	1.3 ± 0.1 (n=3)	34.3 ± 2.3 (n=3)	0.25
M1-186 H190-243	1.3 ± 0.06 (n=3)	3.5 ± 0.5 (n=3)	2.1	1.5 ± 0.1 (n=3)	6.06 ± 1.0 (n=3)	1.7

^a The cellular cholesterol released from J774 cells to 20 $\mu\text{g/ml}$ of WT human apo A-I was $9 \pm 3 \%$ /4 h (n=21) (mean \pm SD), and all V_{max} values are normalized to this value.

^b The catalytic efficiency (V_{max}/K_m) for WT human apo A-I- mediated efflux from J774 cells was $1.6 \pm 0.5 \%$ FC efflux (4h)⁻¹ ($\mu\text{g apo/ml}$)⁻¹ (mean \pm SD) and all catalytic efficiencies are normalized to this value.

^c The cellular cholesterol released from BHK cells to 20 $\mu\text{g/ml}$ of WT human apoA-I was $28 \pm 4\%$ /4h (n=12) and all of V_{max} values are normalized to this value.

^d The catalytic efficiency (V_{max}/K_m) for WT human apoA-I-mediated efflux from BHK cells was $4.2 \pm 0.6 \%$ FC efflux (4h)⁻¹ ($\mu\text{g apo/ml}$)⁻¹ and all catalytic efficiencies are normalized to this value.

Table 2 Sizes of nascent HDL particles formed by ABCA1-expressing BHK cells incubated with different apo A-I domains

Apolipoprotein	Human apo A-I			Mouse apo A-I			Domain swaps	
	Res 1-243	Res 1-189	Res 190-243	Res 1-240	Res 1-186	Res 187-240	Human 1-189 Mouse 187-240	Mouse 1-186 Human 190-243
Peak diameters of particles formed (nm)	8	-	-	-	-	a	-	8
	10	14	10	11	12.5		12	10

^a No HDL formed

Figure 1

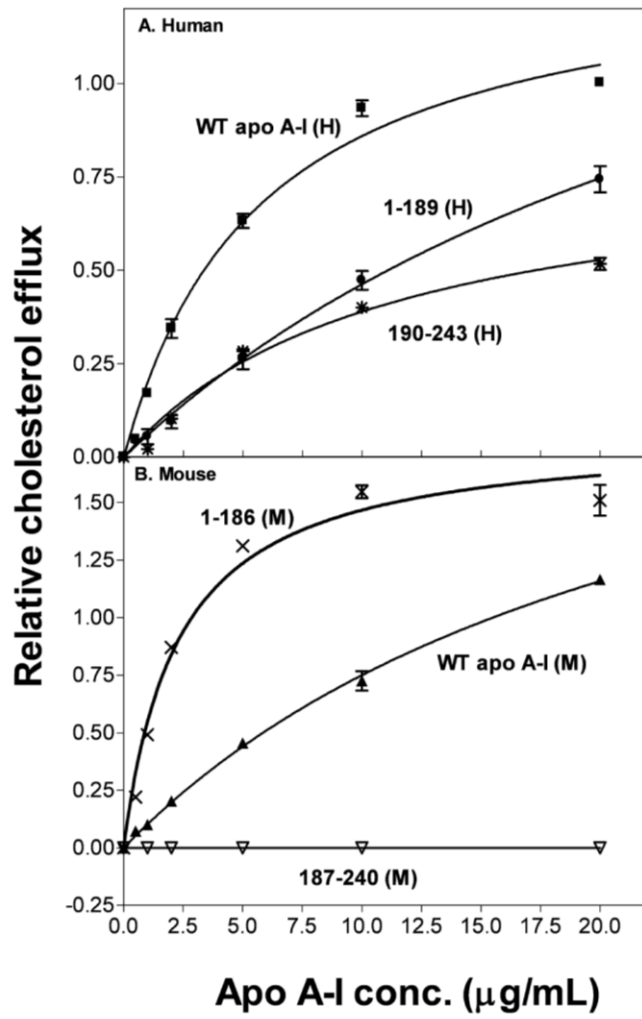


Figure 2

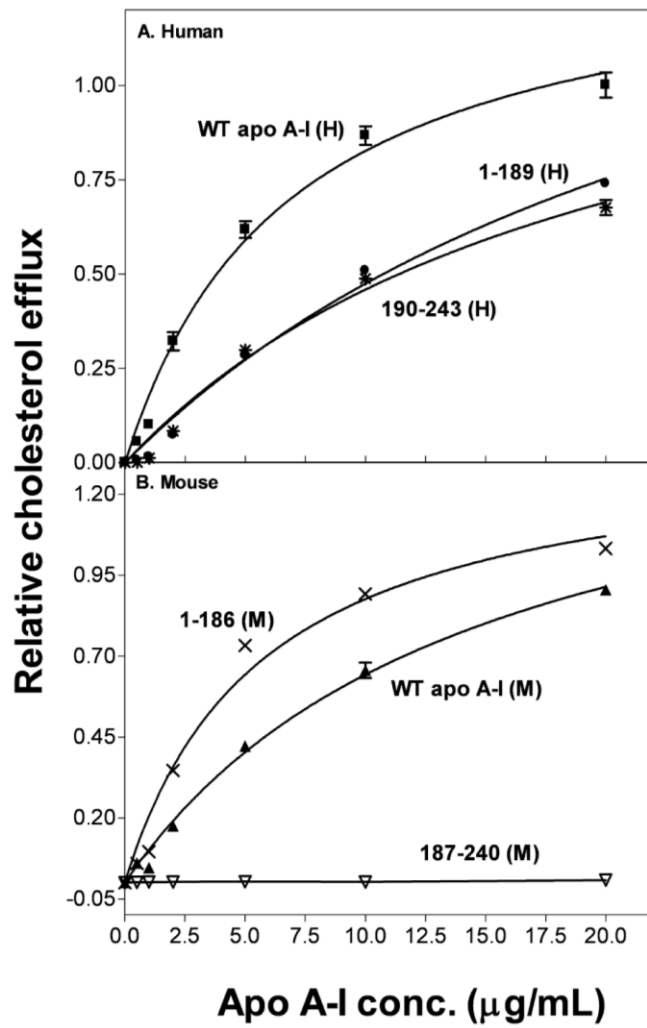


Figure 3

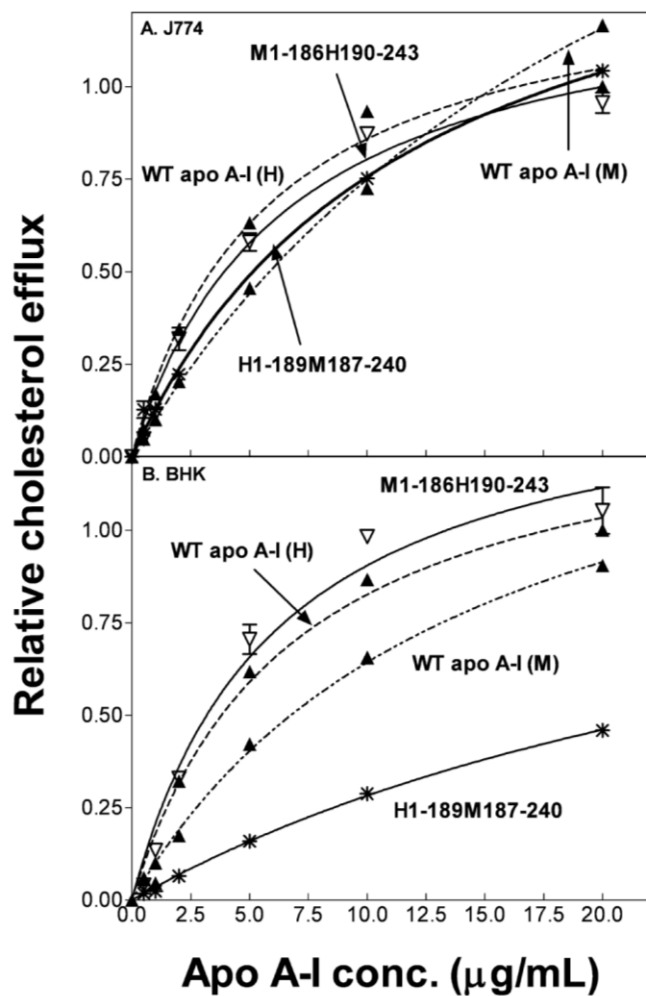


Figure 4

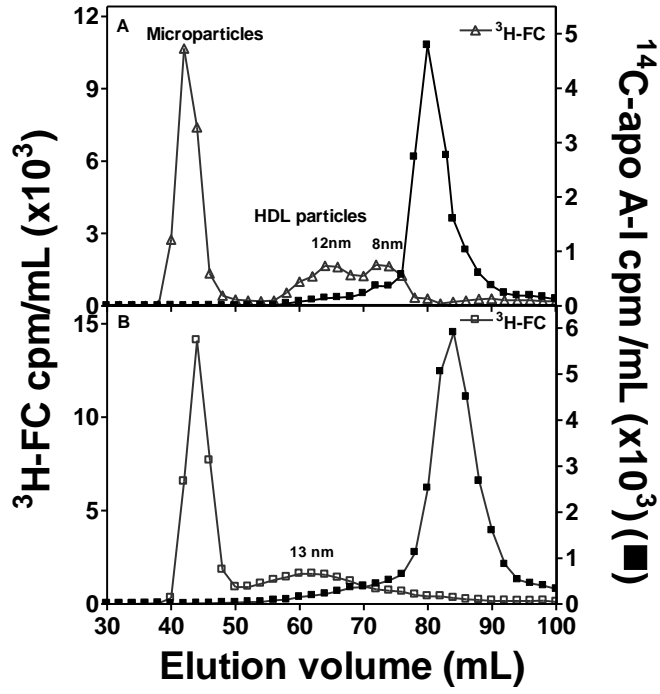


Figure 5

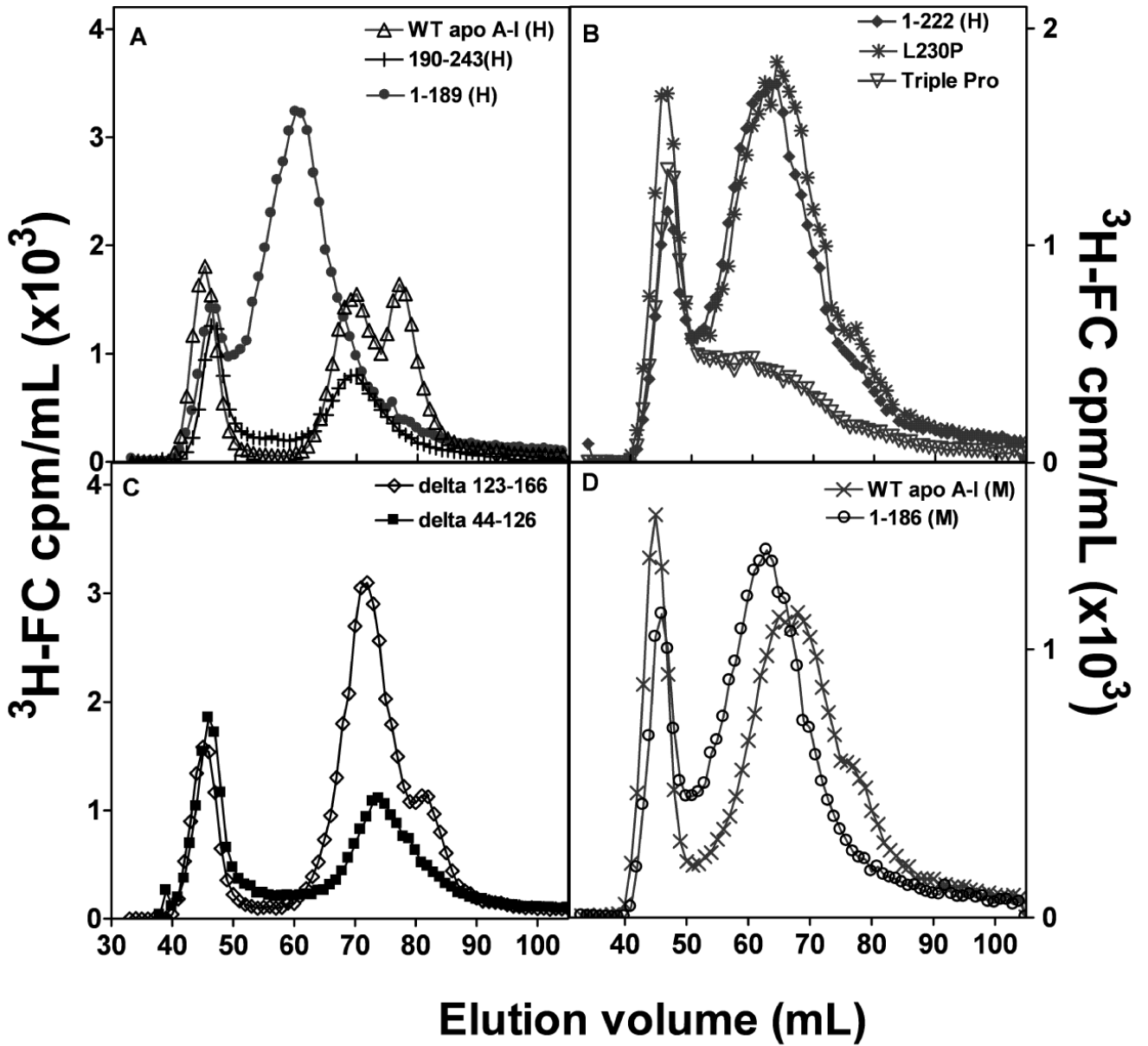


Figure 6

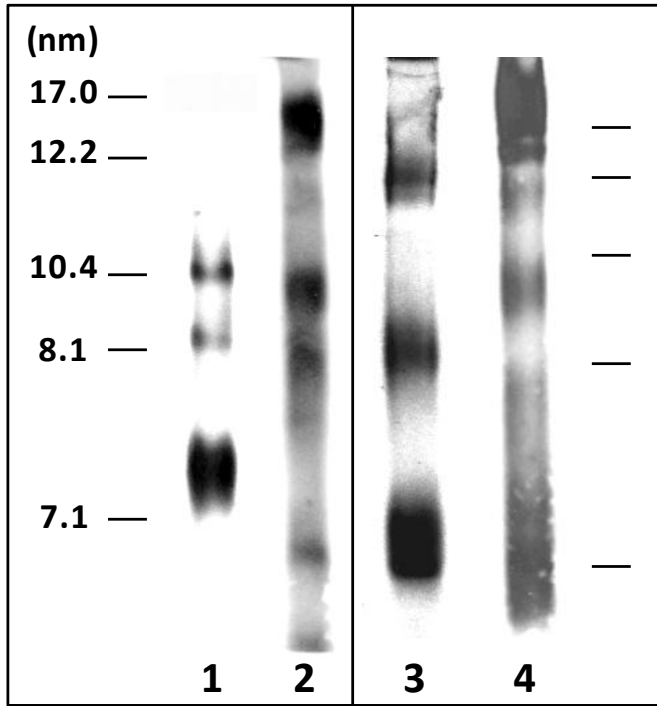


Figure 7

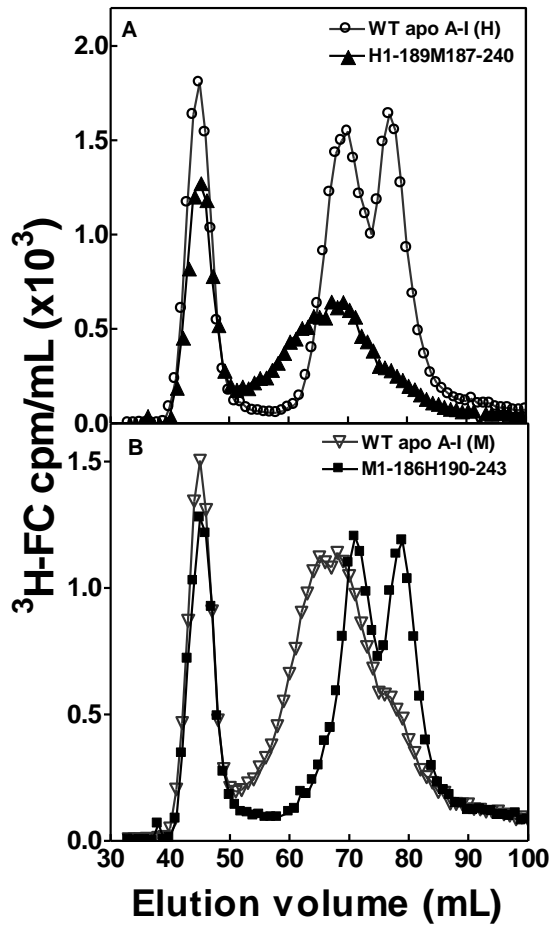
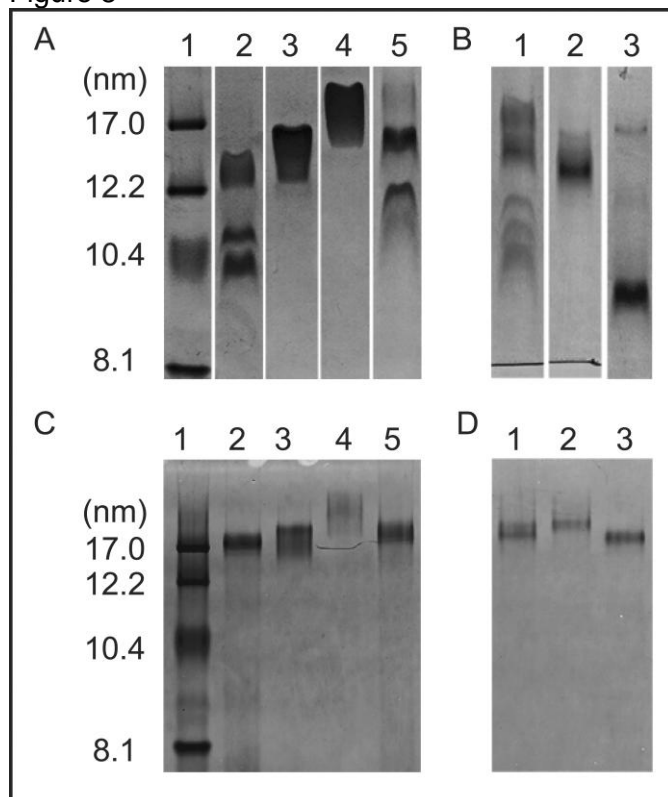
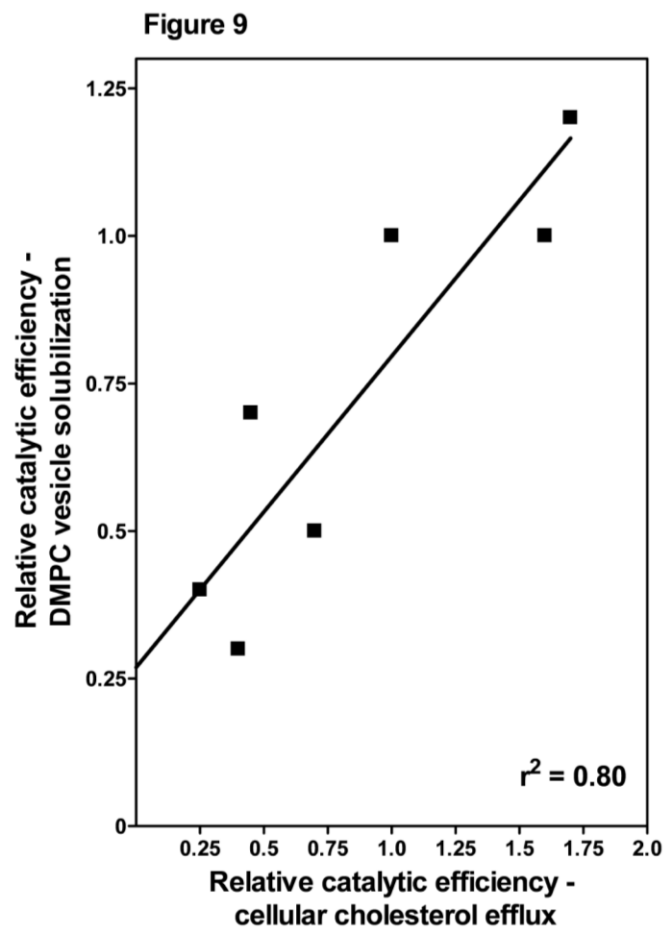


Figure 8





Influence of apolipoprotein (APO) A-I structure on nascent high density lipoprotein (HDL) particle size distribution

Charulatha Vedhachalam, Palaniappan Sevugan Chetty, Margaret Nickel, Padmaja Dhanasekaran, Sissel Lund-Katz, George H. Rothblat and Michael C. Phillips

J. Biol. Chem. published online August 2, 2010

Access the most updated version of this article at doi: [10.1074/jbc.M110.126292](https://doi.org/10.1074/jbc.M110.126292)

Alerts:

- [When this article is cited](#)
- [When a correction for this article is posted](#)

[Click here](#) to choose from all of JBC's e-mail alerts

This article cites 0 references, 0 of which can be accessed free at <http://www.jbc.org/content/early/2010/08/02/jbc.M110.126292.full.html#ref-list-1>